Giedraityte, Zivile; Tuomisto, Minnea; Lastusaari, Mika; Karppinen, Maarit

# Three- and Two-Photon NIR-to-Vis (Yb,Er) Upconversion from ALD/MLD-Fabricated Molecular Hybrid Thin Films

*Published in:*
ACS Applied Materials and Interfaces

*DOI:*
10.1021/acsami.7b19303

Published: 14/03/2018

*Document Version*
Peer reviewed version

*Please cite the original version:*
Giedraityte, Z., Tuomisto, M., Lastusaari, M., & Karppinen, M. (2018). Three- and Two-Photon NIR-to-Vis (Yb,Er) Upconversion from ALD/MLD-Fabricated Molecular Hybrid Thin Films. ACS Applied Materials and Interfaces, 10(10), 8845-8852. https://doi.org/10.1021/acsami.7b19303

# Three- and Two-Photon NIR-to-vis (Yb,Er) Upconversion from ALD/MLD Fabricated Molecular Hybrid Thin Films

Zivile Giedraityte,[1,#] Minnea Tuomisto,[2,3,#] Mika Lastusaari,[2,4] Maarit Karppinen[1,*]

[1] Department of Chemistry and Materials Science, Aalto University, FI-00076 Aalto, Finland

[2] Department of Chemistry, University of Turku, FI-20014 Turku, Finland

[3] Doctoral Programme in Physical and Chemical Sciences, University of Turku Graduate School (UTUGS), Turku, Finland

[4] Turku University Centre for Materials and Surfaces (MatSurf), Turku, Finland

# These authors have contributed equally to this work

*KEYWORDS: upconversion luminescence; inorganic-organic hybrids; thin films; atomic/molecular layer deposition*

ABSTRACT: We report blue, green and red upconversion emissions with strongly angular dependent intensities for new type of hybrid (Y,Yb,Er)-pyrazine thin films realized using the atomic/molecular layer deposition (ALD/MLD) thin-film fabrication technology. The luminescence emissions in our amorphous (Y,Yb,Er)-pyrazine thin films of a controllable nanothickness originate from three- and two-photon NIR-to-vis excitation processes. In addition to shielding the lanthanide ions from nonradiative de-excitation, the network of interconnected organic molecules serves as an excellent matrix for the $Yb^{3+}$-to-$Er^{3+}$ excitation energy transfer. This suggests a new approach to achieve efficient upconverting molecular materials with the potential for *e.g.* next-generation medical diagnostics, waveguides and surface-sensitive detectors.

## 1. INTRODUCTION

Photon upconversion is a phenomenon where lower energy photons are piled up to create higher energy photons.[1] This can be achieved by using lanthanide ions with suitable energy levels, *i.e.* those that possess energy level ladders with appropriate steps. For upconversion from near-infrared (NIR) to the visible light the most efficient ion is $Er^{3+}$, which alone is capable of upconversion luminescence. When $Yb^{3+}$ sensitization for the $Er^{3+}$ emission is used, even higher emission efficiencies may be obtained. Another possibility to achieve upconversion is by triplet-triplet annihilation in organic molecules, but then the conversion is limited to the visible range only.[2] Upconversion materials are currently intensely studied in particular for application in medical diagnostics and imaging to replace the traditional $Eu^{3+}$ and $Tb^{3+}$ based photoluminescence markers.[3-5] Upconversion is preferred over the regular photoluminescence because it allows excitation in the optical transparency window of the tissue, thus preventing the undesirable autofluorescence. Once the autofluorescence can be avoided there is no need for the time-resolved measurements that are required for the $Eu^{3+}$ and $Tb^{3+}$ markers.

The current state-of-the-art upconverters are inorganic nanocrystals. Unfortunately, application of such nanocrystals in diagnostics is strongly limited by the availability of right-sized nanocrystals as well as the difficulties in their dispersibility to liquid media and surface functionalization. In comparison with the present inorganic upconverters, molecular metal complexes could offer much higher sensitivities in bioapplications. This is because in the upconverting molecular materials all the optically active sites can be brought to the close proximity with the biologically active ligands, while in the inorganic nanocrystals this is the case only for the active sites on the very surface of the crystals. However, a nearly surmountable challenge with the molecular upconverters has been the remarkably strong nonradiative relaxation of excitation in metal complexes caused by the high-energy phonons of the ligands.[6]

There are some successful works though, reporting the direct NIR-to-vis upconversion in lanthanide complexes. In these relatively rare examples the nearly impossible has been made possible by ensuring that (i) each emitter has enough sensitizers in the close vicinity, (ii) the sensitizers' excited states have long enough lifetimes for energy transfer, and (iii) the emitter is protected from the high-energy vibrations.[7] Aboshyan-Sorgho *et al.*[7] reported $Cr^{3+}$-sensitized NIR-to-vis upconversion from $Er^{3+}$ in a molecular trinuclear complex. The emission was however observed only at low temperatures where the impact of multiphonon relaxation could be minimized. On the other hand, Suffren *et al.*[8] as well as Zare *et al.*[9] realized $Cr^{3+}$-sensitized NIR-to-green $Er^{3+}$ upconversion from multinuclear complexes even at room temperature; according to the authors the

successive excitation photons were stored by $Cr^{3+}$ before the transfer to $Er^{3+}$. Blackburn *et al.*[10] reported room-temperature two-photon upconversion for $Tm^{3+}$-based complexes in $d^6$-DMSO solutions, and Xiao *et al.*[11] for $Nd(EDTA)_2^{5-}$, $Er(DPA)_3^{3-}$ and $Tm(DPA)_3^{3-}$ complexes, but only with a very high-power (100 kW) excitation. Hyppänen *et al.*[12] showed NIR-to-green upconversion for ion-associated $Er(TTA)_4$ in the presence of the IR-806 molecule as an absorber. Suzuki *et al.*[13] obtained green-to-UV upconversion in Er(III)tris(8-hydroxyquinoline) at room temperature, and Yang *et al.*[14] reported the same for $[Nd_2(NDC)_3(DMF)_4]\times H_2O$. Furthermore, Weng *et al.*[15] showed two-phonon NIR-to-green and NIR-to-red upconversions in dinuclear (Yb,Er)-based metal-organic frameworks, but the red emission was highly weakened by the presence of $OH^-$ groups. Interestingly, Sun *et al.*[16] reported even upconversion from NIR to blue in single crystals of $[(Y:Er\text{-}Yb)(oba)(ox)_{0.5}(H_2O)_2]_n$. Unfortunately, neither Weng *et al*.[15] nor Sun *et al*.[16] gave details of the measurement conditions such as the excitation power or temperature. However, recently Nonat *et al.*[17] reported NIR-to-green and NIR-to-red room-temperature upconversion from fluorinated dinuclear $Er^{3+}$ complexes. They used $D_2O$ as the solvent and a rather low-power (5 W) laser. There are also a few reports of lanthanide luminescence after upconversion in organic ligands, see *e.g.* Wong *et al*.[18] and Luo *et al*.[19]

An attractive new way of synthesizing inorganic-organic hybrid materials is provided by the currently strongly emerging atomic/molecular layer deposition (ALD/MLD) thin-film technique.[20-24] The technique has the capacity to yield novel hybrid materials with unique bonding schemes and molecular assemblies not readily accessible with any other synthesis technique. There are already exciting examples of functional properties discovered for such ALD/MLD-fabricated thin films relevant to next-generation thermoelectric,[25,26] Li-ion microbattery,[27] encapsulation,[28,29] and metal organic framework[30,31] applications. Most importantly, the ALD/MLD fabrication of lanthanide-based inorganic-organic photoluminescence thin films has also been demonstrated.[32,33]

The ALD/MLD technique is derived from the state-of-the-art gas-phase thin-film deposition technique of simple inorganic materials, *i.e*. ALD (atomic layer deposition), developed for industrial-scale applications already in 1970s.[34] An example of the industrial feasibility of ALD is the fabrication of ultrathin $HfO_2$ gate dielectrics coatings for microprocessors. For the inorganic-organic thin films, ALD cycles are combined with MLD (molecular layer deposition) cycles based on an organic precursor. This enables the atomic/molecular layer-by-layer growth of inorganic-organic hybrid thin films through sequential self-limiting gas-surface reactions of gaseous precursor pulses with high precision for the film thickness and composition. The ALD/MLD technology has several other inherent advantages highly relevant to advanced upconversion applications in *e.g.* medical diagnostics, such as the possibility to use the technique for (sub)nano-scale surface functionalization of various complex surface architectures,[35,36] and low-temperature deposition of flexible hybrid coatings on sensitive or demanding substrates such as polymers, textiles[37] or biomaterials.[38] Very recently we reported the ALD growth of highly homogeneous upconverting inorganic $(Yb,Er)_2O_3$ thin films.[39] In the present work, we demonstrate for the first time the NIR-to-vis lanthanide upconversion emission for ALD/MLD fabricated molecular inorganic-organic thin films. We chose pyrazine as the ligand for the (Y,Yb,Er) complex, because it has been shown to form stable complexes[40] and upconverting metal-organic frameworks[41] with lanthanides. Most importantly revealed is that: (i) the emission shows all the three red-green-blue (RGB) main colors including the most-difficult-to-obtain blue color, (ii) these are achieved with both three- and two-photon processes, and (iii) the emission intensity is highly angle-dependent. The latter observation is extremely intriguing for application in ultra-sensitive fluorescence assays and surface sensors for point-of care diagnostics.[42-46]

## 2. EXPERIMENTAL SECTION

*Thin-film depositions*: We selected the following metal composition for our upconverting hybrid thin films: 0.92 Y, 0.04 Yb and 0.04 Er. For the organic component, we used pyrazine carboxylate. The thin-film samples were fabricated in a commercial ALD reactor (F-120 by ASM Microchemistry Ltd.) from our in-house synthesized[30,47] mixed $(Y_{0.92}Yb_{0.04}Er_{0.04})(thd)_3$ metal precursor and commercial 2,3-pyrazinedicarboxylic acid powder (Sigma Aldrich) as the organic precursor. During the depositions, the $(Y,Yb,Er)(thd)_3$ and pyrazinedicarboxylic acid precursor powders were kept in glass crucibles inside the reactor at 130 and 145 °C, respectively. Nitrogen (>99.999%; Schmidilin UHPN 3000 $N_2$ generator) was used as a carrier and purging gas, and a pressure of 2 to 4 mbar was maintained in the reactor during the film deposition. The following ALD/MLD precursor pulse / purge cycle was repeated for 150 times: 1.5 s $(Y,Yb,Er)(thd)_3$ / 2 s $N_2$ / 2 s pyrazine / 4 s $N_2$. The depositions were carried out at different temperatures in the range of 160-250 °C on various substrates: silicon(100), DuPont polyimide, quartz and nanocellulose.

*Characterization*: Thickness, density and roughness of the films were determined by X-ray reflectivity (XRR; Panalytical X'Pert MPD Pro Alfa 1) measurements using XPERT HighScore Plus-reflectivity. Grazing incidence X-ray diffraction (GIXRD) measurements were done using the same instrument. The organic content was confirmed and the bonding scheme investigated using Fourier transform infrared spectroscopy (FTIR; Nicolet Magna-IR Spectrometer 750), where an average of 32 scans with 4 $cm^{-1}$ resolution was applied for each sample. UV–visible absorption spectroscopy PerkinElmer Lambda 950 UV/Vis/NIR absorption spectrophotometer was used for the absorbance measurements. Surface morphology was investigated with atomic force microscopy (AFM; Veeco Dimension 51000 Scanning Probe Microscope; Nanoscope Controller, Digital Instruments, Inc.; Nanoscope Analysis 1.5 Software). The Y:Yb:Er content was confirmed from X-ray fluorescence (XRF)

spectrometer (XRF; PANalytical AxiosmaX with a Rh tube, 3 kW model) data.

The upconversion measurements were carried out using Avaspec-HS-TEC CCD spectrometer and Optical Fiber Systems IFC-975-008 NIR laser (6W, 974 nm). In the excitation path, a 900 nm long-pass filter (Edmund Optics) was used to cut off wavelengths lower than NIR. The emitted light was collected at 90° angle to the excitation and directed through a 900 nm filter (Newport, 10SWF-900-B) to exclude the scattered excitation radiation. An optical fiber with 600 µm diameter was used as an emission light path between the sample compartment and the detector. All spectra were measured at room temperature.

## 3. RESULTS AND DISCUSSION

First we demonstrate that our ALD/MLD process for the (Y,Yb,Er)-pyrazine thin films from (Y,Yb,Er)(thd)$_3$ and pyrazinedicarboxylic acid precursors works in the expected ideal atomic/molecular layer-by-layer deposition mode. This can be seen from Figures 1(a) and 1(b), where we show that the growth-per-cycle (GPC) remains essentially constant independent of the precursor pulse lengths, and the film thickness increases in a linear manner with increasing number of ALD/MLD cycles. These experiments were carried out on silicon substrates at 160 °C. We also nvestigated higher deposition temperatures up to 280 °C. From Figure 1(c) it is seen that the GPC remains essentially constant up to 225 °C, then slightly declines for 250-280 °C possibly due to (partial) decomposition of the pyrazinedicarboxylic acid precursor. At all the deposition temperatures the resultant thin films were visually homogeneous. Thus, we may conclude that our (Y,Yb,Er)(thd)$_3$ + pyrazine dicarboxylic acid ALD/MLD process yields high-quality thin films through self-limiting gas-surface reactions of the precursors with the selected ALD/MLD parameters in the deposition temperature range of 160–225 °C. For the rest of the depositions we selected the following precursor/purge sequence: 1.5 s (Y,Yb,Er)(thd)$_3$ / 2 s $N_2$ / 2 s pyrazine / 4 s $N_2$, and fixed the deposition temperature to 160 °C which is low enough for the temperature-sensitive substrates as well. With these parameters the GPC value was found to be 3.4 Å/cycle such that e.g. 60 and 150 ALD/MLD cycles resulted in ca. 20-nm and 50-nm thick films, respectively; these 20 – 50 nm thick films were investigated in all our further experiments. From XRR and AFM measurements (not shown here) the roughness of the films was determined to be 0.2 nm; the density value calculated from the XRR data was 2.0 g/cm$^3$. From GIXRD the films were found amorphous up to 250 °C; only raising the deposition temperature to 275 °C resulted in some crystallinity, see Figure 1(d).

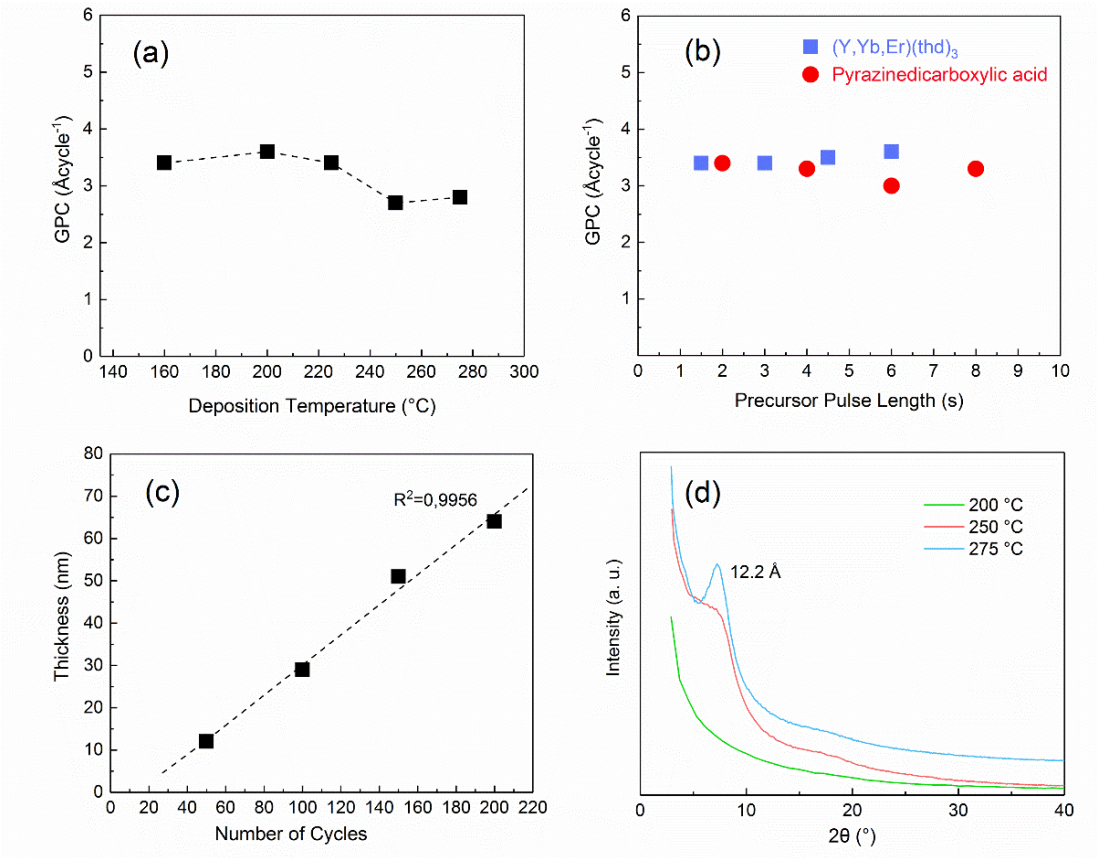


Figure 1. Optimization of the ALD/MLD film growth parameters: (a) growth-per-cycle (GPC) as a function of deposition temperature (150 ALD/MLD cycles) (b) GPC as a function of precursor pulse lengths (deposition temperature 160 °C, 150 ALD/MLD cycles), and (c) film thickness as a function of the number of ALD/MLD cycles (deposition temperature 160 °C). (d) GIXRD patterns for thin films grown at 200-275 °C.

Next we discuss the chemical state of our (Y,Yb,Er)-pyrazine thin films based on an FTIR investigation, see Figure 2(a,b) where the spectrum recorded for the hybrid thin film is compared to that of the pyrazine dicarboxylic acid precursor. The features seen in the latter spectrum are all well explained by the literature data for 2,3-pyrazinedicarboxylic acid;[48] the assignment of the major features is shown in Figure 2(a,b). Then, comparison of the spectrum for the (Y,Yb,Er)-pyrazine thin film to that of the pyrazine dicarboxylic acid precursor reveals that the COOH bands observed for the precursor at 1754, 1715 and 1681 $cm^{-1}$ due to $\nu$(C=O), at 3265 and 2843-2489 $cm^{-1}$ due to $\nu(OH^-)$, and at 1263, 766 and 677 $cm^{-1}$ due to β (HOC) and β(OCO),[48-49] are completely missing for the hybrid thin film, proving that – as expected – the metal cations are bound to the organic molecule via these groups to form (Y,Yb,Er)-oxygen bonds. On the other hand, for the hybrid thin film new bands appear due to asymmetric and symmetric stretching vibrations of the carboxylate group: $\nu_{as}(COO^-)$ at 1611 $cm^{-1}$ and $\nu_s(COO^-)$ in the 1390-1366 $cm^{-1}$ range.[49] The difference, $\Delta_{coo} = \nu_{as}(COO^-) - \nu_s(COO^-)$, is 245 $cm^{-1}$, which implies that the metal-carboxylate bond is of the unidentante type.[50] In addition, new bands appear at 609 and 562 $cm^{-1}$; these are due to (Y,Yb,Er)-O stretching modes.[51] Another important observation is that instead of the CN bands, observed in the pyrazine dicarboxylic acid precursor at 1577-1482 $cm^{-1}$, a new band appears at 1448 $cm^{-1}$ for the hybrid thin film, suggesting that the metal cations most likely are bonded to the pyrazine molecule via nitrogen atoms as well. Moreover, the stretching mode $\nu$(CH) at 3096 $cm^{-1}$ as well as the bending modes β(CH) of aromatic ring observed at 1208, 1182, 994, and 868 $cm^{-1}$ in the spectrum of the 2,3-pyrazinedicarboxylic acid, are missing in the spectrum of the hybrid thin film. These changes in the charge distribution of the aromatic ring are due to 2,3-pyrazinedicarboxylic acid-metal interactions.[52] Based on all the aforementioned observations, we present a possible 2D bonding scheme for our hybrid (Y,Yb,Er)-pyrazine thin films in Figure 2(d).

The UV/vis absorption spectrum obtained for the films is shown in Figure 2(c) together with that for the pyrazine dicarboxylic acid precursor. The pure precursor spectrum shows the well-known transitions at 212 nm due to H-2-L (68%) and at 268 and 318 nm due to H-L (96%) and (H-L+1 (96%)) transitions.[48] Upon the (Y,Yb,Er)-pyrazine complex formation the absorption wavelength shifts from 268 nm to 290 nm; similar shifts have been seen in related metal complexes and ascribed to ligand-to-metal charge transfer.[53-56] Additionally, new weak peaks appear at 1384 and 2210 nm; these most probably originate from the metal-ligand interaction.

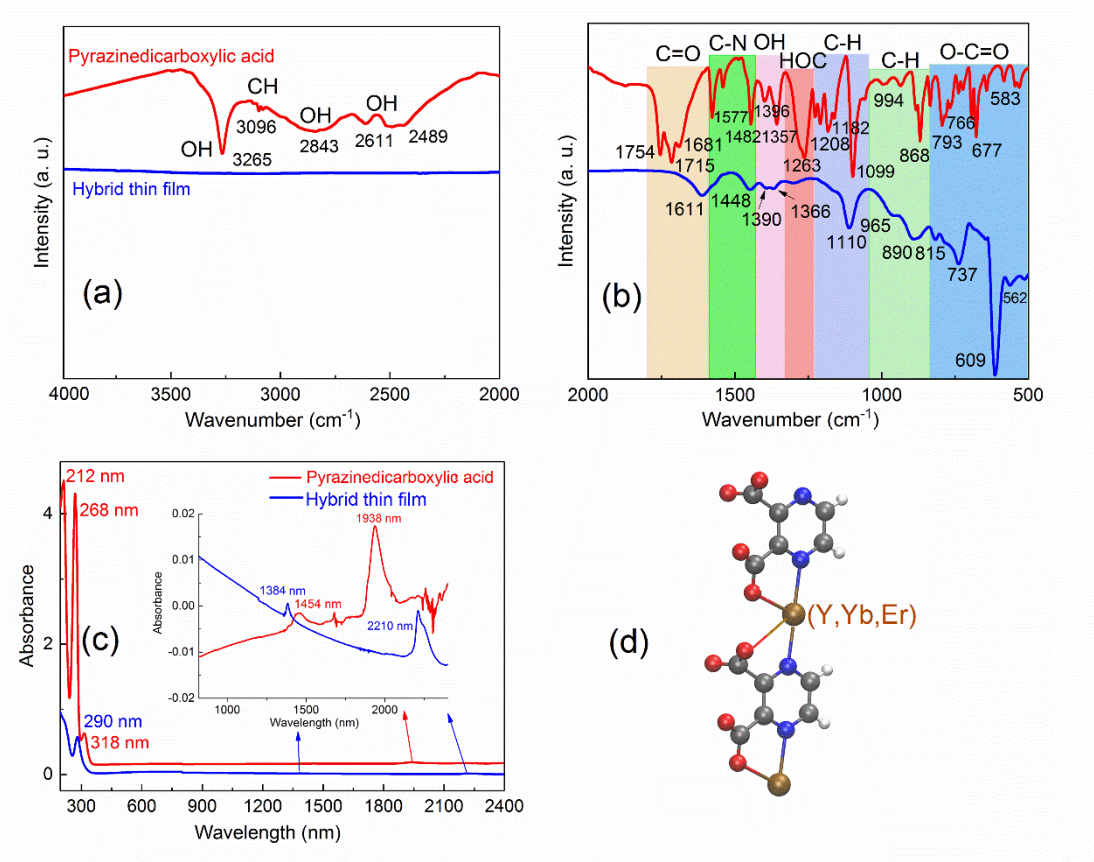


Figure 2. (a,b) FTIR spectra for our hybrid (Y,Yb,Er)-pyrazine thin film and the pyrazine-2,3-carboxylic acid precursor, and (c) UV-vis-NIR-absorption spectrum for the same (Y,Yb,Er)-pyrazine thin-film sample. (d) Possible bonding scheme based on the FTIR data.

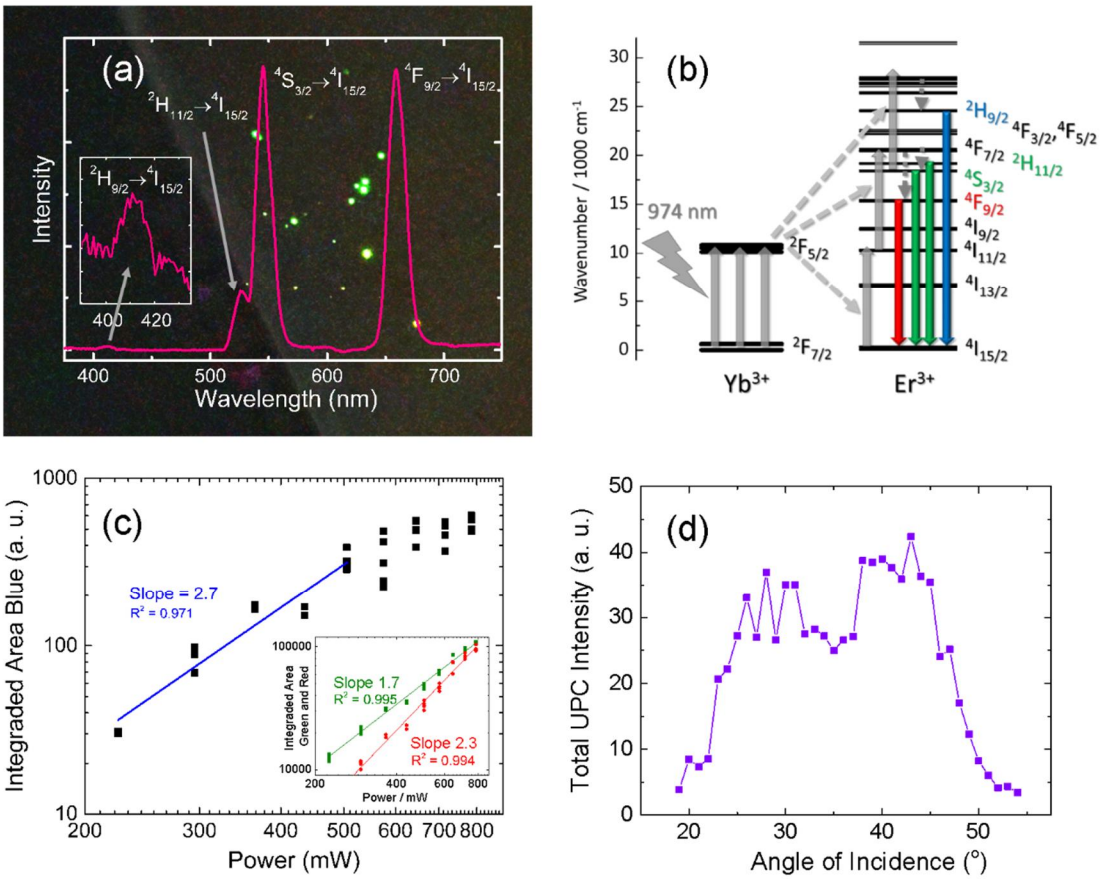


Figure 3. (a) Upconversion emission spectrum for a representative (Y,Yb,Er)-pyrazine thin film grown on Si substrate. The background shows a composite image of the film excited at 974 nm in different spots (taken through a NIR blocking filter). (b) A schematic presentation of the up-conversion mechanism. (c) Laser pump power dependencies for the (Y,Yb,Er)-pyrazine thin film, and (d) dependence of the UPC emission intensity on the incident angle of excitation.

As for the characterization of the upconversion properties, we first investigated several hybrid thin films grown on silicon, which is a rigid substrate thus allowing easy upconversion characterization. We initially prepared a series of thin films with different thicknesses from 20 to 50 nm to check the possible effect of the film thickness on the upconversion; within this thickness range the upconversion intensity was confirmed to be essentially independent of the film thickness. The films were excited with 974 nm radiation and they showed green and red upconversion emissions that are due to the $^2H_{11/2}$,$^4S_{3/2}\rightarrow{}^4I_{15/2}$ and $^4F_{9/2}\rightarrow{}^4I_{15/2}$ transitions of $Er^{3+}$, respectively (Figure 3(a)). The fact that the films show excellent upconversion emission intensity indicates that the ALD/MLD process has enabled the build-up of a structure with close $Yb^{3+}$-$Er^{3+}$ pairs enabling the efficient energy transfer and a shielding of the energy transfer and relaxation processes from the vibrations of the ligands. As the (Y,Yb,Er)-pyrazine thin films were found to exhibit a weak absorption band in the NIR range (Figure 2(b)), we tentatively believe that the ligands may absorb the 974 nm excitation and transfer it to $Yb^{3+}$ and $Er^{3+}$ thus enhancing the up-conversion process further.

A striking new feature for the (Yb,Er) upconversion in molecular compounds is that the present films show also the blue emission of $Er^{3+}$ due to the $^2H_{9/2}\rightarrow{}^4I_{15/2}$ transition (Figure 3(a)). To the best of our knowledge, there are no reports on NIR-to-blue emissions in amorphous molecular compounds yet. This is because the blue lines require a pile-up of three photons in the upconversion process (Figure 3 (b)) and its probability is much lower than that of the two-phonon processes. In molecular complexes, the probability is made even lower due to the vibrations of the ligands that act as efficient pathways for multiphonon de-excitation.

The upconversion emission intensity is known to be dependent on the pump excitation power,[57] and therefore we carried out the pump power measurements. Moreover, the laser wavelength is dependent on the temperature of the laser and therefore the temperature affects the effectiveness of excitation. To account for this, we measured a few spectra per each pump power using different cooling powers for the laser. Upconversion is a multiphoton absorption process which means that the up-conversion intensity and pump power have an exponential dependence.[58] At low excitation powers, a linear fitting of the log-log dependence between the intensity and pump power will give a slope which corresponds to the number of photons needed for the upconversion process. As shown in Figure 3(c), for our

(Y,Yb,Er)-pyrazine thin film the slope of the blue emission is 2.7, which indicates a three-photon process, as expected. For the green emission the slope is 1.7, which is in agreement with a two-photon process, see e.g. ref. 59. For the red emission, the slope is 2.3 which may indicate a three-photon process with some leaking pathways during the photon pile-up or it may be a two-photon process as discussed in the literature.[60-63] The plot of NIR-to-blue emission shows also a decrease of slope at the highest pump excitation powers. This is caused by an excitation power induced change in the net excited-state dynamics due to increasing excitation photon density.[64] The blue emission can be thought to be more strongly affected by this than the green or red ones, because it requires more energy-climbing steps to succeed, *i.e.* small changes in the first two steps accumulate to bigger ones in the third step. The saturation of sensitized upconversion emission has been reported and discussed in more detail in earlier literature, see *e.g.* refs. 64,65. All in all, as proven by Suyver *et al*.[62] the saturation indicates that the upconversion emission in our films is not due to the direct excitation of $Er^{3+}$ but with a process involving sensitization via $Yb^{3+}$ ions.

We investigated also the red/green upconversion emission intensity ratios for the power series of our (Y,Yb,Er)-pyrazine films. The results show that the red emission intensity increases relatively more than the green emission when the excitation power increases, *i.e.* we observed a linear rise from 0.43 red/green ratio at 0.23 W to 0.90 at 0.79 W with a slope of 0.85. This is important, as it is known that the red emission is more important than the green one in bioapplications owing to its better ability to penetrate tissues.[66,67] Because we observed no excitation power dependent saturation for neither emission, this observed increase in the red/green ratio is due to the increase of the temperature along the increasing excitation power; as can be seen from the energy level diagram depicted in Figure 2(d), the energy differences between the $^2H_{11/2}$, $^4S_{3/2}$, $^4F_{9/2}$ and $^4I_{11/2}$ levels are much smaller than those between $^4I_{11/2}$, $^4I_{13/2}$ and $^4I_{15/2}$. Therefore, increasing temperature will increase the multiphonon de-excitation probability of the green emitting $^2H_{11/2}$, $^4S_{3/2}$ levels much more efficiently than that of the red-emitting $^4I_{11/2}$ level.

We also tested the dependence of the incident angle of the laser beam on the upconversion emission intensity. Because of the finite thickness of thin films, they will show an excitation angle dependence of emission intensity because of effects such as excitation photon density and penetration depth that have no influence in bulk luminescent materials. Angular dependencies for thin film luminescence have been presented in *e.g.* refs. 68-70 and typically the intensity varies with angle, but there is still emission from all angles. However, for our film, the upconversion emission is obtained only with incident angles between ca. 20 and 50 degrees, as demonstrated in Figure 3(d). Such a narrow angular range is something that is typical of surface plasmon coupled emission.[71] Thanks to this narrow angular range with or without possible surface plasmon contribution, we envision that our films could be used as *e.g.* waveguides and surface-sensitive detectors.

Finally, inspired by the excellent results for the films deposited on silicon, we fabricated (Y,Yb,Er)-pyrazine thin films on transparent and flexible polyimide and nanocellulose substrates. Also these films show the green and red upconversion emissions (Figure 4). The log-log dependence of the intensity and pump excitation power present slopes of 1.4 (green) and 1.5 (red) for the films on the polyimide substrate and 1.3 (green) and 2.1 (red) for those on the nanocellulose substrate (not shown here). Thus, both upconversion processes can be taken to be two-photon processes. Accordingly, the red/green ratios for the cases of the polyimide and nanocellulose substrates are somewhat lower than those for the films grown on silicon. Tentatively, we believe that the small difference could be just due to slightly different random distributions of the $Yb^{3+}$ and $Er^{3+}$ cations. Nevertheless, the results confirm the excellent upconversion performance of our molecular (Y,Yb,Er)-pyrazine upconverting thin films on different surfaces enabled by the ALD/MLD fabrication protocol.

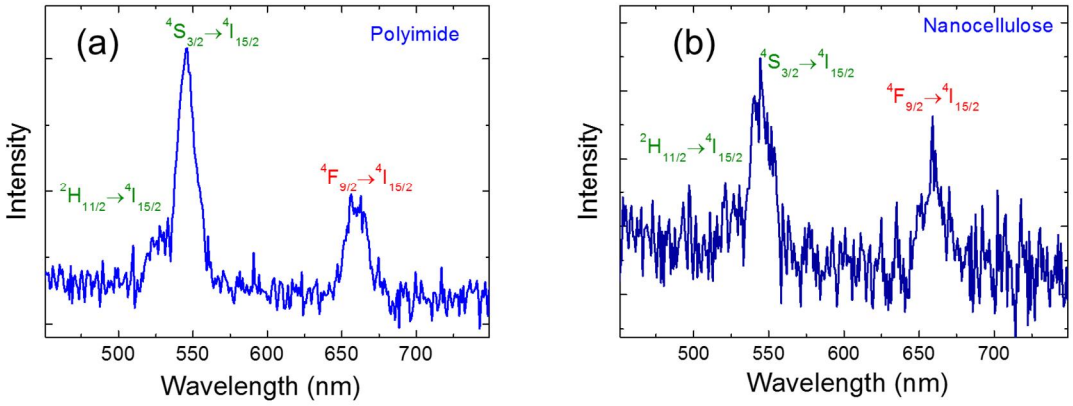


Figure 4. Upconversion emission spectra for (Y,Yb,Er)-pyrazine thin films deposited on flexible (a) polyimide and (b) nanocellulose substrates.

## 4. CONCLUSIONS

Molecular metal-complex upconverters would be exciting material candidates for application in *e.g.* medical diagnostics to replace the traditional photoluminescence markers, as they allow excitation in the optical transparency window of the tissue such that the problematic autofluorescence of the tissue can be avoided. However, the nonradiative relaxation of excitation caused by the high-energy phonons of the ligands in typical metal complexes so far investigated has remained an almost surmountable challenge for the realization of such otherwise ideal upconverting materials.

In this work, we have demonstrated that our new type of (Y,Yb,Er)-based hybrid inorganic-organic thin-film materials synthesized using the strongly emerging ALD/MLD technique can overcome the aforementioned challenge. We showed that these hybrid thin films allow both two- and three-photon processes to yield upconversion luminescence emissions with all the three RGB main colors including the most-difficult-to-obtain blue color. Also very interestingly, the emission intensities were found to be highly angle-dependent.

Although further studies are definitely required the novel inorganic-organic thin-film materials precisely fabricated using the ALD/MLD technique could open up interesting application possibilities in *e.g.* bioanalytics and medical diagnostics; note that the ALD/MLD technique inherently brings several advantageous properties for the films including the excellent integratibility with various substrate surfaces as demonstrated in the present work. Our proof-of-the-concept results are for (Y,Yb,Er)-pyrazine thin films. We however envision that further tuning/optimization of the upconversion characteristics could be achieved by systematically mapping various organic constituents in the (Y,Yb,Er)-organic complex.

## ACKNOWLEDGEMENTS

This work has received funding from the European Research Council under the European Union's Seventh Framework Programme (FP/2007-2013)/ERC Advanced Grant Agreement (No. 339478), Academy of Finland (No. 296299) and the Fortum Foundation. Kari Loikas and Mauri Nauma (University of Turku, Department of Chemistry) are thanked for constructing the upconversion emission measurement and photo setup.

References


1. Auzel, F. Upconversion and Anti-Stokes Processes with f and d Ions in Solids. *Chem. Rev. (Washington, DC, U. S. )* 2004, *104*, 139-173.

2. Zhou, J.; Liu, Q.; Feng, W.; Sun, Y.; Li, F. Upconversion Luminescent Materials: Advances and Applications. *Chem. Rev. (Washington, DC, U. S. )* 2015, *115*, 395-465.

3. Zhou, L.; Wang, R.; Yao, C.; Li, X.; Wang, C.; Zhang, X.; Xu, C.; Zeng, A.; Zhao, D.; Zhang, F. Single-band upconversion nanoprobes for multiplexed simultaneous in situ molecular mapping of cancer biomarkers. *Nat. Commun.* 2015, *6*, 6938.

4. Wang, F.; Deng, R.; Wang, J.; Wang, Q.; Han, Y.; Zhu, H.; Chen, X.; Liu, X. Tuning upconversion through energy migration in core-shell nanoparticles. *Nat. Mater.* 2011, *10*, 968-973.

5. Liu, Y.; Lu, Y.; Yang, X.; Zheng, X.; Wen, S.; Wang, F.; Vidal, X.; Zhao, J.; Liu, D.; Zhou, Z.; Ma, C.; Zhou, J.; Piper, J. A.; Xi, P.; Jin, D. Amplified stimulated emission in upconversion nanoparticles for super-resolution nanoscopy. *Nature (London, U. K. )* 2017, *543*, 229-233.

6. Reinhard, C.; Guedel, H. U. High-Resolution Optical Spectroscopy of Na3[Ln(dpa)3]Â·13H2O with Ln = Er3+, Tm3+, Yb3+. *Inorg. Chem.* 2002, *41*, 1048-1055.

7. Aboshyan-Sorgho, L.; Besnard, C.; Pattison, P.; Kittilstved, K. R.; Aebischer, A.; Buenzli, J. G.; Hauser, A.; Piguet, C. Near-Infraredâ†'Visible Light Upconversion in a Molecular Trinuclear d-f-d Complex. *Angew. Chem. , Int. Ed.* 2011, *50*, 4108-4112, S4108/1-S4108/34.

8. Suffren, Y.; Zare, D.; Eliseeva, S. V.; Guenee, L.; Nozary, H.; Lathion, T.; Aboshyan-Sorgho, L.; Petoud, S.; Hauser, A.; Piguet, C. Near-Infrared to Visible Light-Upconversion in Molecules: From Dream to Reality. *J. Phys. Chem. C* 2013, *117*, 26957-26963.

9. Zare, D.; Suffren, Y.; Guenee, L.; Eliseeva, S. V.; Nozary, H.; Aboshyan-Sorgho, L.; Petoud, S.; Hauser, A.; Piguet, C. Smaller than a nanoparticle with the design of discrete polynuclear molecular complexes displaying near-infrared to visible upconversion. *Dalton Trans.* 2015, *44*, 2529-2540.

10. Blackburn, O. A.; Tropiano, M.; Sorensen, T. J.; Thom, J.; Beeby, A.; Bushby, L. M.; Parker, D.; Natrajan, L. S.; Faulkner, S. Luminescence and upconversion from thulium(III) species in solution. *Phys. Chem. Chem. Phys.* 2012, *14*, 13378-13384.

11. Xiao, X.; Haushalter, J. P.; Faris, G. W. Upconversion from aqueous phase lanthanide chelates. *Opt. Lett.* 2005, *30*, 1674-1676.

12. Hyppanen, I.; Lahtinen, S.; Aaritalo, T.; Makela, J.; Kankare, J.; Soukka, T. Photon Upconversion in a Molecular Lanthanide Complex in Anhydrous Solution at Room Temperature. *ACS Photonics* 2014, *1*, 394-397.

13. Suzuki, H.; Nishida, Y.; Hoshino, S. Ligand-sensitized and up-conversion photoluminescence in vacuum-deposited thin films of an infrared electroluminescent organic erbium complex. *Mol. Cryst. Liq. Cryst.* 2003, *406*, 221-231.

14. Yang, J.; Yue, Q.; Li, G.; Cao, J.; Li, G.; Chen, J. Structures, photoluminescence, up-conversion, and magnetism of 2D and 3D rare-earth coordination polymers with multicarboxylate linkages. *Inorg Chem* 2006, *45*, 2857-2865.

15. Weng, D.; Zheng, X.; Chen, X.; Li, L.; Jin, L. Synthesis, upconversion luminescence and magnetic properties of new lanthanide-organic frameworks with (43)2(46,66,83) topology. *Eur. J. Inorg. Chem.* 2007, 3410-3415.

16. Sun, C.; Zheng, X.; Chen, X.; Li, L.; Jin, L. Assembly and upconversion luminescence of lanthanide-organic frameworks with mixed acid ligands. *Inorg. Chim. Acta* 2009, *362*, 325-330.

17. Nonat, A.; Chan, C. F.; Liu, T.; Platas-Iglesias, C.; Liu, Z.; Wong, W.; Wong, W.; Wong, K.; Charbonniere, L. J. Room temperature molecular up conversion in solution. *Nat. Commun.* 2016, *7*, 11978.

18. Wong, K.; Kwok, W.; Wong, W.; Phillips, D. L.; Cheah, K. Green and red three-photon upconversion from polymeric lanthanide(III) complexes. *Angew. Chem. , Int. Ed.* 2004, *43*, 4659-4662.

19. Luo, L.; Lai, W. P.; Wong, K.; Wong, W.; Li, K.; Cheah, K. Green upconversion fluorescence in terbium coordination complexes. *Chem. Phys. Lett.* 2004, *398*, 372-376.

20. Klepper, K. B.; Nilsen, O.; Hansen, P.; Fjellvag, H. Atomic layer deposition of organic-inorganic hybrid materials based on saturated linear carboxylic acids. *Dalton Trans.* 2011, *40*, 4636-4646.

21. George, S. M. Atomic Layer Deposition: An Overview. *Chem. Rev. (Washington, DC, U. S. )* 2010, *110*, 111-131.

22. Sundberg, P.; Karppinen, M. Organic and inorganic-organic thin film structures by molecular layer deposition: A review. *Beilstein J. Nanotechnology* 2014, *5*, 1104-1136.

23. Gregorczyk, K.; Knez, M. Hybrid nanomaterials through molecular and atomic layer deposition: Top down, bottom up, and in-between approaches to new materials. *Prog. Mater. Sci.* 2016, *75*, 1-37.

24. Van Bui, H.; Grillo, F.; van Ommen, J. R. Atomic and molecular layer deposition: off the beaten track. *Chem. Commun. (Cambridge, U. K. )* 2017, *53*, 45-71.

25. Tynell, T.; Terasaki, I.; Yamauchi, H.; Karppinen, M. Thermoelectric characteristics of (Zn,Al)O/hydroquinone superlattices. *J. Mater. Chem. A* 2013, *1*, 13619-13624.

26. Tynell, T.; Giri, A.; Gaskins, J.; Hopkins, P. E.; Mele, P.; Miyazaki, K.; Karppinen, M. Efficiently suppressed thermal conductivity in ZnO thin films via periodic introduction of organic layers. *J. Mater. Chem. A* 2014, *2*, 12150-12152.

27. Nisula, M.; Karppinen, M. Atomic/Molecular Layer Deposition of Lithium Terephthalate Thin Films as High Rate Capability Li-Ion Battery Anodes. *Nano Lett.* 2016, *16*, 1276-1281.

28. Vaha-Nissi, M.; Sundberg, P.; Kauppi, E.; Hirvikorpi, T.; Sievanen, J.; Sood, A.; Karppinen, M.; Harlin, A. Barrier properties of Al2O3 and alucone coatings and nanolaminates on flexible biopolymer films. *Thin Solid Films* 2012, *520*, 6780-6785.

29. Xiao, W.; Hui, D. Y.; Zheng, C.; Yu, D.; Qiang, Y. Y.; Ping, C.; Xiang, C. L.; Yi, Z. Flexible transparent gas barrier film employing the method of mixing ALD/MLD-grown Al2O3 and alucone layers. *Nanoscale Res. Lett.* 2015, *10*, 1-7.

30. Ahvenniemi, E.; Karppinen, M. Atomic/molecular layer deposition: a direct gas-phase route to crystalline metal-organic framework thin films. *Chem. Commun. (Cambridge, U. K. )* 2016, *52*, 1139-1142.

31. Ahvenniemi, E.; Karppinen, M. In Situ Atomic/Molecular Layer-by-Layer Deposition of Inorganic-Organic Coordination Network Thin Films from Gaseous Precursors. *Chem. Mater.* 2016, *28*, 6260-6265.

32. Giedraityte, Z.; Sundberg, P.; Karppinen, M. Flexible inorganic-organic thin film phosphors by ALD/MLD. *J. Mater. Chem. C* 2015, *3*, 12316-12321.

33. Giedraityte, Z.; Johansson, L. -.; Karppinen, M. ALD/MLD fabrication of luminescent Eu-organic hybrid thin films using different aromatic carboxylic acid components with N and O donors. *RSC Adv.* 2016, *6*, 103412-103417.

34. Puurunen, R. L. A Short History of Atomic Layer Deposition: Tuomo Suntola's Atomic Layer Epitaxy. *Chem. Vap. Deposition* 2014, *20*, 332-344.

35. Ghosal, S.; Baumann, T. F.; King, J. S.; Kucheyev, S. O.; Wang, Y.; Worsley, M. A.; Biener, J.; Bent, S. F.; Hamza, A. V. Controlling Atomic Layer Deposition of TiO2 in Aerogels through Surface Functionalization. *Chem. Mater.* 2009, *21*, 1989-1992.

36. Ritter, H.; Nieminen, M.; Karppinen, M.; Bruehwiler, D. A comparative study of the functionalization of mesoporous silica MCM-41 by deposition of 3-aminopropyltrimethoxysilane from toluene and from the vapor phase. *Microporous Mesoporous Mater.* 2009, *121*, 79-83.

37. Karttunen, A. J.; Sarnes, L.; Townsend, R.; Mikkonen, J.; Karppinen, M. Flexible Thermoelectric ZnO-Organic Superlattices on Cotton Textile Substrates by ALD/MLD. *Adv. Electron. Mater.* 2017, *3*, n/a.

38. Malm, J.; Sahramo, E.; Karppinen, M.; Ras, R. H. A. Photo-Controlled Wettability Switching by Conformal Coating of Nanoscale Topographies with Ultrathin Oxide Films. *Chem. Mater.* 2010, *22*, 3349-3352.

39. Tuomisto, M.; Giedraityte, Z.; Karppinen, M.; Lastusaari, M. Photon up-converting (Yb,Er)2O3 thin films by atomic layer deposition. *Phys. Status Solidi RRL* 2017, *11*, n/a.

40. Zheng, X.; Ablet, A.; Ng, C.; Wong, W. Intensive Upconversion Luminescence of Na-Codoped Rare-Earth Oxides with a Novel RE-Na Heterometallic Complex as Precursor. *Inorg. Chem.* 2014, *53*, 6788-6793.

41. Suffren, Y.; Golesorkhi, B.; Zare, D.; Guenee, L.; Nozary, H.; Eliseeva, S. V.; Petoud, S.; Hauser, A.; Piguet, C. Taming Lanthanide-Centered Upconversion at the Molecular Level. *Inorg. Chem.* 2016, *55*, 9964-9972.

42. Nayak, S.; Blumenfeld, N. R.; Laksanasopin, T.; Sia, S. K. Point-of-Care Diagnostics: Recent Developments in a Connected Age. *Anal. Chem. (Washington, DC, U. S. )* 2017, *89*, 102-123.

43. Petryayeva, E.; Algar, W. R. Toward point-of-care diagnostics with consumer electronic devices: the expanding role of nanoparticles. *RSC Adv.* 2015, *5*, 22256-22282.

44. Valta, T.; Kale, V.; Soukka, T.; Horn, C. Near-infrared excited ultraviolet emitting upconverting phosphors as an internal light source in dry chemistry test strips for glucose sensing. *Analyst (Cambridge, U. K. )* 2015*, 140*, 2638-2643.

45. Juntunen, E.; Arppe, R.; Kalliomaki, L.; Salminen, T.; Talha, S. M.; Myyrylainen, T.; Soukka, T.; Pettersson, K. Effects of blood sample anticoagulants on lateral flow assays using luminescent photon-upconverting and Eu(III) nanoparticle reporters. *Anal Biochem* 2016*, 492*, 13-20.

46. Widejko, R.; Wang, F.; Anker, J. In *In Development of pressure sensing particles through SERS and Upconversion.* 2011; , pp SERM-662.

47. Eisentraut, K. J.; Sievers, R. E. Volatile rare-earth chelates of 2,2,6,6-tetramethylheptane-3,5-dione. *Inorg. Synth.* 1968*, 11*, 94-98.

48. Bhat, S. A.; Faizan, M.; Alam, M. J.; Ahmad, S. Vibrational and electronic spectral analysis of 2,3-pyrazinedicarboxylic acid: A combined experimental and theoretical study. *Spectrosc. Lett.* 2016*, 49*, 449-457.

49. Soares-Santos, P. C. R.; Cunha-Silva, L.; Almeida Paz, F. A.; Ferreira, R. A. S.; Rocha, J.; Carlos, L. D.; Nogueira, H. I. S. Photoluminescent Lanthanide-Organic Bilayer Networks with 2,3-Pyrazinedicarboxylate and Oxalate. *Inorg. Chem.* 2010*, 49*, 3428-3440.

50. Gribble, G. W.; Joule, J. A.; Editors Progress In Heterocyclic Chemistry, Volume 21. 2009, 559.

51. Repelin, Y.; Proust, C.; Husson, E.; Beny, J. M. Vibrational spectroscopy of the C-form of yttrium sesquioxide. *J. Solid State Chem.* 1995*, 118*, 163-169.

52. Swiderski, G.; Lewandowska, H.; Swislocka, R.; Wojtulewski, S.; Siergiejczyk, L.; Wilczewska, A. Thermal, spectroscopic (IR, Raman, NMR) and theoretical (DFT) studies of alkali metal complexes with pyrazinecarboxylate and 2,3-pyrazinedicarboxylate ligands. *J. Therm. Anal. Calorim.* 2016*, 126*, 205-224.

53. Truillet, C.; Lux, F.; Brichart, T.; Lu, G. W.; Gong, Q. H.; Perriat, P.; Martini, M.; Tillement, O. Energy transfer from pyridine molecules towards europium cations contained in sub 5-nm Eu2O3 nanoparticles: Can a particle be an efficient multiple donor-acceptor system?. *J. Appl. Phys. (Melville, NY, U. S. )* 2013*, 114*, 114308/1-114308/10.

54. Senegas, J.; Bernardinelli, G.; Imbert, D.; Buenzli, J. G.; Morgantini, P.; Weber, J.; Piguet, C. Connecting Terminal Carboxylate Groups in Nine-Coordinate Lanthanide Podates: Consequences on the Thermodynamic, Structural, Electronic, and Photophysical Properties. *Inorg. Chem.* 2003*, 42*, 4680-4695.

55. Trivedi, E. R.; Eliseeva, S. V.; Jankolovits, J.; Olmstead, M. M.; Petoud, S.; Pecoraro, V. L. Highly Emitting Near-Infrared Lanthanide "Encapsulated Sandwich" Metallacrown Complexes with Excitation Shifted Toward Lower Energy. *J. Am. Chem. Soc.* 2014*, 136*, 1526-1534.

56. Feng, J.; Zhang, H. Hybrid materials based on lanthanide organic complexes: a review. *Chem. Soc. Rev.* 2013*, 42*, 387-410.

57. Pollnau, M.; Gamelin, D. R.; Luthi, S. R.; Gudel, H. U.; Hehlen, M. P. Power dependence of upconversion luminescence in lanthanide and transition-metal-ion systems. *Phys. Rev. B: Condens. Matter Mater. Phys.* 2000*, 61*, 3337-3346.

58. Hewes, R. A.; Sarver, J. F. Infrared excitation processes for the visible luminescense of erbium (III), holmium(III), and thulium(III) in ytterbium(III) sensitized rare-earth trifluorides. *Phys. Rev.* 1969*, 182*, 427-436.

59 . Shang, X.; Chen, P.; Jia, T.; Feng, D.; Zhang, S.; Sun, Z.-M.; Qiu, J. Upconversion luminescence mechanisms of $Er^{3+}$ ions under excitation of an 800 nm laser, *Phys. Chem. Chem. Phys*. 2015, *17*, 11481-11489.

60. Auzel, F. E. Materials and devices using double-pumped phosphors with energy transfer. *Proc. IEEE* 1973*, 61*, 758-786.

61. Xu, D.; Liu, C.; Yan, J.; Yang, S.; Zhang, Y. Understanding Energy Transfer Mechanisms for Tunable Emission of Yb3+-Er3+ Codoped GdF3 Nanoparticles: Concentration-Dependent Luminescence by Near-Infrared and Violet Excitation. *J. Phys. Chem. C* 2015*, 119*, 6852-6860.

62. Berry, M. T.; May, P. S. Disputed Mechanism for NIR-to-Red Upconversion Luminescence in NaYF4:Yb3+,Er3+. *J. Phys. Chem. A* 2015*, 119*, 9805-9811.

63. Shin, K.; Jung, T.; Lee, E.; Lee, G.; Goh, Y.; Heo, J.; Jung, M.; Jo, E.-J.; Lee, H.; Kim, M.-G. Lee, K.T. Distinct mechanisms for the upconversion of $NaYF_4$:$Yb^{3+}$,$Er^{3+}$ nanoparticles revealed by stimulated emission depletion, *Phys. Chem. Chem. Phys*. 2017, *19*, 9739-9744.

64. Suyver, J. F.; Aebischer, A.; Garcia-Revilla, S.; Gerner, P.; Gudel, H. U. Anomalous power dependence of sensitized upconversion luminescence. *Phys. Rev. B:*

*Condens. Matter Mater. Phys.* 2005, *71*, 125123/1-125123/9.

65. Mai, H.; Zhang, Y.; Sun, L.; Yan, C. Highly Efficient Multicolor Up-Conversion Emissions and Their Mechanisms of Monodisperse NaYF4:Yb,Er Core and Core/Shell-Structured Nanocrystals. *J. Phys. Chem. C* 2007, *111*, 13721-13729.

66. Jacques, S. L. Optical properties of biological tissues: a review. *Phys Med Biol* 2013, *58*, R37-61.

67. Kuningas, K.; Pakkila, H.; Ukonaho, T.; Rantanen, T.; Lovgren, T.; Soukka, T. Upconversion fluorescence enables homogeneous immunoassay in whole blood. *Clin. Chem. (Washington, DC, U. S. )* 2007, *53*, 145-146.

68. Gao, R.; Lei, X.; Chen, M.; Yan, D.; Wei, M. Two-color polarized emission and angle-dependent luminescence based on layer-by-layer assembly of binary chromophores/layered double hydroxide thin films. *New J. Chem.* 2013, *37*, 4110-4118.

69. Pan, S. S.; Ye, C.; Teng, X. M.; Li, G. H. Angle-dependent photoluminescence of [1 1 0]-oriented nitrogen-doped SnO2 films. *J. Phys. D: Appl. Phys.* 2007, *40*, 4771-4774.

70. Marra, D. C.; Aydil, E. S.; Joo, S. -.; Yoon, E.; Srdanov, V. I. Angle-dependent photoluminescence spectra of hydrogenated amorphous silicon thin films. *Appl. Phys. Lett.* 2000, *77*, 3346-3348.

71. Cao, S.; Cai, W.; Liu, Q.; Li, Y. Surface plasmon-coupled emission: what can directional fluorescence bring to the analytical sciences?. *Annu. Rev. Anal. Chem.* 2012, *5*, 317-336.

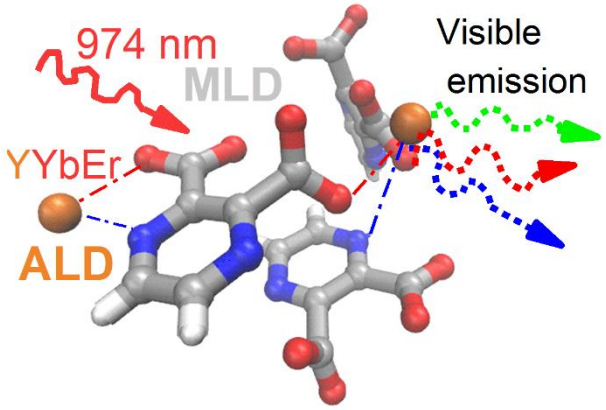


Insert Table of Contents artwork here